Supporting Information

Biomimetic multi-functional superamphiphobic FOTS-TiO_2 particles beyond lotus leaf

Liwei Chen,[a,b] Zhiguang Guo*[a,b] and Weimin Liu[b]

[a] Hubei Collaborative Innovation Centre for Advanced Organic Chemical Materials and Ministry of Education Key Laboratory for the Green Preparation and Application of Functional Materials, Hubei University, Wuhan 430062, China.

[b] State Key Laboratory of Solid Lubrication, Lanzhou Institute of Chemical Physics, Chinese Academy of Sciences, Lanzhou 730000, China.

Fax: +86-931-8277088; Tel: +86-931-4968105; E-mail: zguo@licp.cas.cn

1. Schematic illustrating the application methods

With its own superamphiphobic property, the flower-like FOTS-TiO_2 powder as surface building blocks for superamphiphobic coating is applicable to various substrates, including hard, soft and fluffy materials. With the assistance of double-sided tape or spray adhesive, the powder can be coated onto the substrates by a flexible method, such as, sift-deposition, spraying, or dip-coating, according to the feature of host substrates.

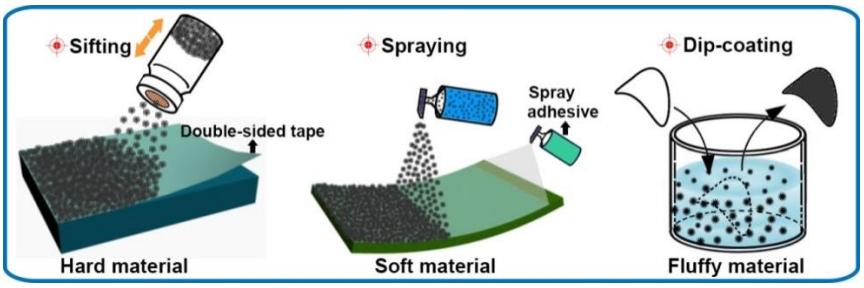

Schematic S1: Schematic illustration of the different methods to bond the superamphiphobic FOTS-TiO_2 powder onto various substrates.

2. Fourier transform infrared spectroscopy (FT-IR) data

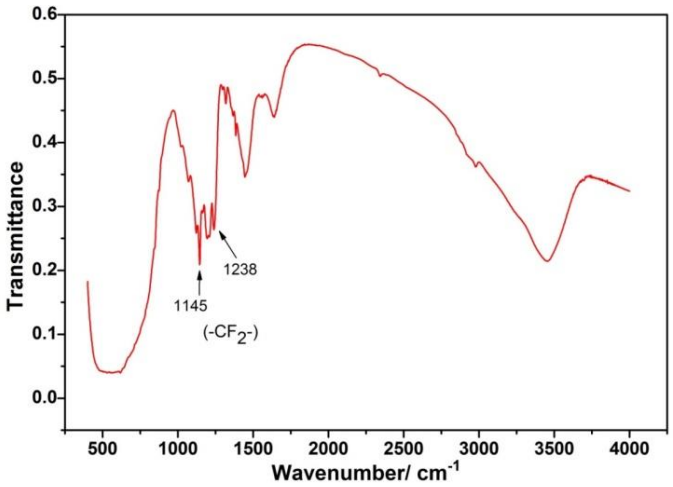

Fig. S1: FT-IR spectra of the FOTS-TiO_2 particles. The typical absorption peaks of function group $-CF_2-$ appear at 1145 cm^{-1} and 1238 cm^{-1}. The appearance of function group $-CF_2-$ is vital to the resulting superamphiphobicity of PFOTS-TiO_2 particles.

3. Thermal gravimetric analysis (TGA) data

To know the thermal stability of the superamphiphobic FOTS-TiO_2 powder, thermal gravimetry (TG) measurements were done with a dynamic heating rate of 10 °C min^{-1} under the atmosphere of nitrogen. The obtained curve indicates that the thermal decomposition starts at 248.4 ℃ and terminates at 371.6 ℃ with TG of 77.1%, showed great thermal stability up to 348 °C.

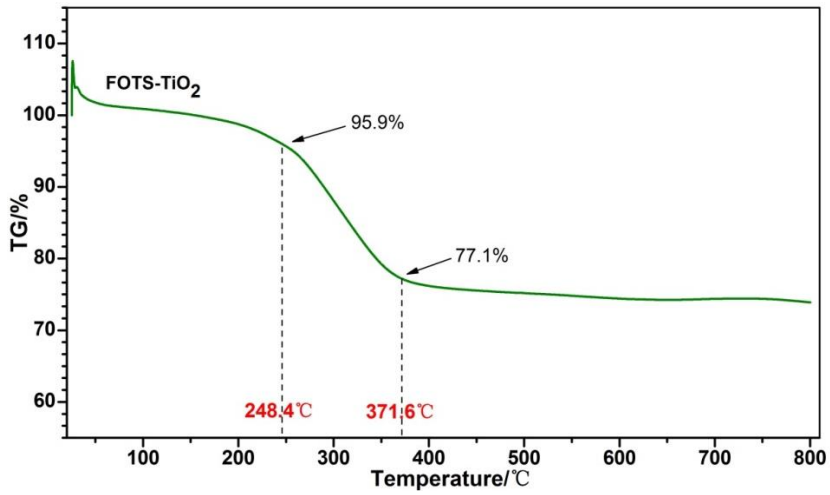

Fig. S2: Thermal gravimetric analysis (TGA) curve of the superamphiphobic FOTS-TiO_2 particles.

4. The range of liquid repellency of the FOTS-TiO_2 powder

To know the range of liquid repellency of the superamphiphobic FOTS-TiO_2 powder, the contact angles (CA) and rolling angles (RA) of various liquid droplets were measured on the pressed powder blocks. Each data was tested for five times to get an average value, as shown in the following Table S1.

Table S1: List of the liquids repelled by the superamphiphobic FOTS-TiO_2 powder.

Liquids	**Surface tension/mN m^{-1}**	**CA/ °**	**RA/ °**
Water			
Water (T_R)	72.8	160.3 ± 1.7°	0.5 ± 0.1°
Water (Hot)		157.7 ± 1.4°	0.9 ± 0.3°
Water (pH=1)		159.0 ± 1.0°	0.7 ± 0.2°
Water (pH=14)		158.9 ± 1.3°	0.8 ± 0.2°
Composite			
Milk		156.3 ± 1.4°	0.9 ± 0.1°
Coffee		158.1 ± 1.1°	0.8 ± 0.4°
Coke		155.0 ± 1.2°	1.2 ± 0.2°
Cooking oils			
Colza oil		152.1 ± 0.9°	4.5 ± 0.7°
Peanut oil	34.5	152.2 ± 0.8°	4.7 ± 0.6°
Organic solvents			
Glycerol	63.6	153.7 ± 2.5°	5.2 ± 0.9°
Ethylene glycol	47.3	157.8 ± 0.9°	2.9 ± 0.4°
Benzyl alcohol	38.0	156.7 ± 2.0°	3.7 ± 0.6°
Diesel oil		153.2 ± 0.5°	2.4 ± 0.4°
1,2-dichloroethane	33.3	150.8 ± 1.4°	4.1 ± 0.7°
n-Hexadecane	27.5	153. 1 ± 0.8°	3.4 ± 0.3°
Cyclohexane	24.95	152.7 ± 1.0°	2.7 ± 0.5°
n-Decane	23.8	152.2 ± 0.6°	2.2 ± 0.3°

5. Example illustrations of various substrates coated with FOTS-TiO_2 powder

5.1. Surface wettability and morphology of coated zinc plate

The host zinc (Zn) plate was pretreated with double-sided mounting tape and bonded with the powder by sift-deposition method. As a result, the testing droplets including water, glycerol, colza oil, cyclohexane and 1, 2-dichloroethane wet the naked Zn plate for the amphiphilic property itself, but kept high contact angles on coated Zn plate for the superamphiphobic property of FOTS-TiO_2 coating. All of the water and oil contact angles on the coated Zn substrate are measured to be above 150°. Top-view SEM images of coated Zn plate showed that the surface was covered by plenty of flower-like FOTS-TiO_2 particles, which formed a lotus-leaf-like multi-level surface morphology.

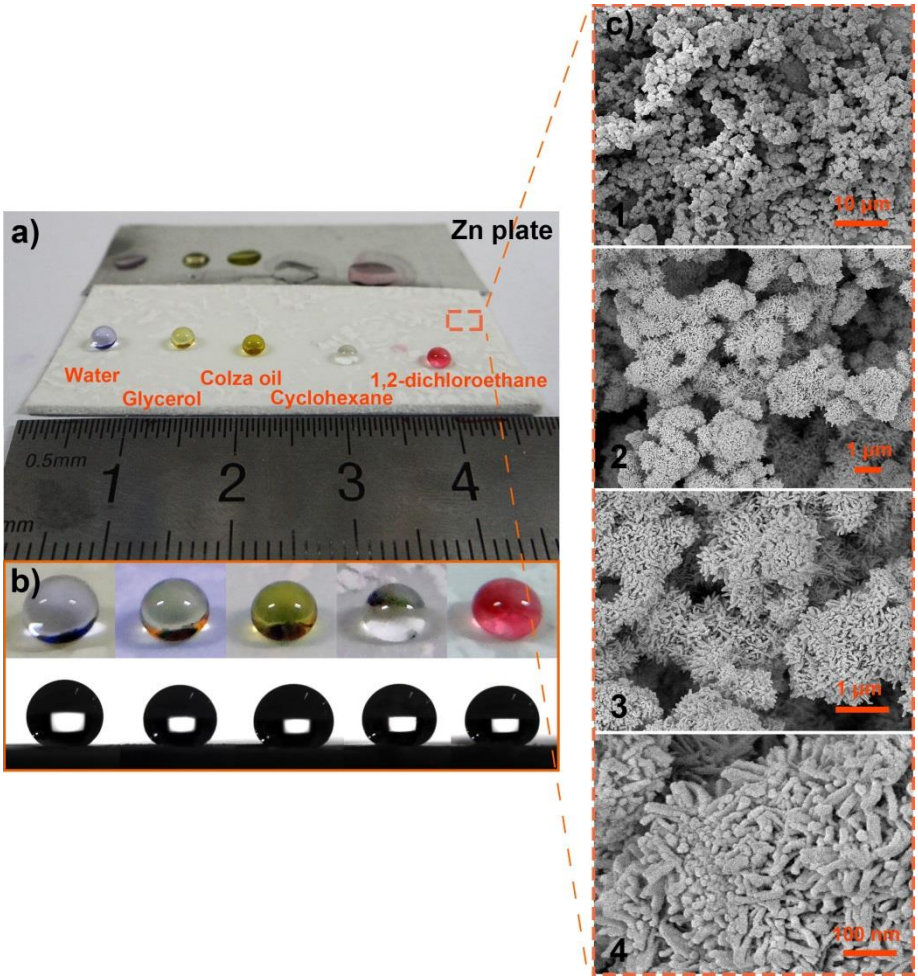

Fig. S3: Superamphiphobicity and surface morphology of FOTS-TiO_2-coated Zn plate. (a) Different surface wettability between uncoated and coated Zn plate. (b) Shape and state of water and oil droplets on the surface of coated Zn plate. The testing droplets are water, glycerol, colza oil, cyclohexane and 1, 2-dichloroethane, orderly. (c_{1-4}) Top-view SEM images of coated Zn plate.

5.2. Surface morphologies of initial and coated filter papers

The host filter paper was pre-treated with spray adhesive and bonded with the powder by sift-deposition method. It is worth noting that the spray adhesive is inherently hydrophobic and the water contact angle approaches 90°. In the top-view SEM images, one can see that the surface of naked filter paper is composed of messy dendritic fibers but relatively smooth, while the surface of coated filter paper is rough and covered with plenty of flower-like FOTS-TiO_2 particles.

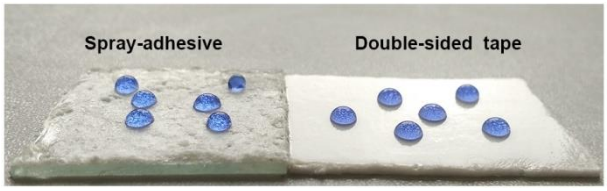

Fig. S4: The water-repellent property of used spray adhesive and double-sided tape.

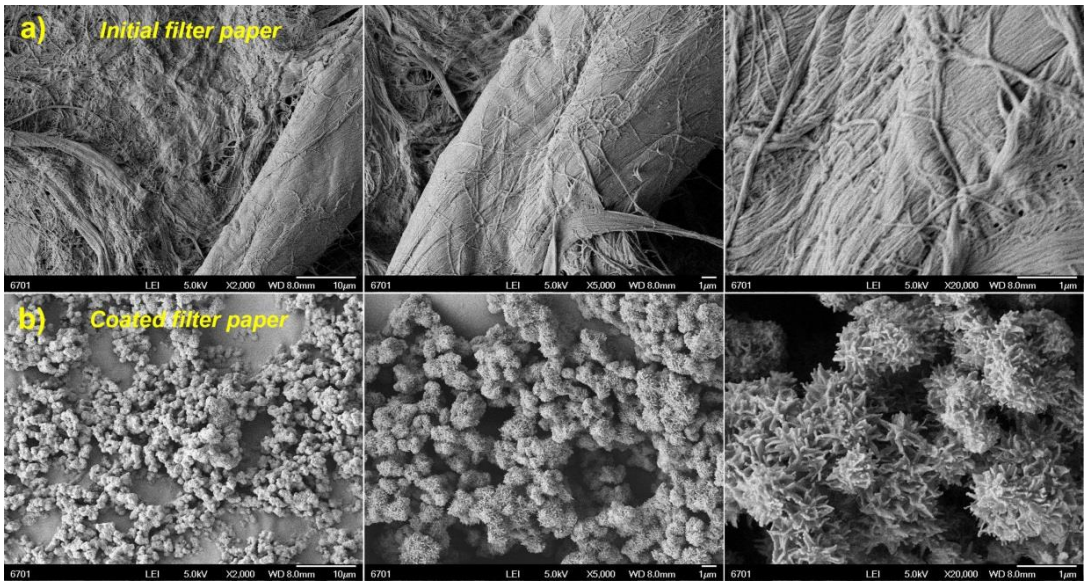

Fig. S5: Top-view SEM images of (a) initial and (b) FOTS-TiO_2-coated filter papers.

5.3. Surface morphologies of initial and coated PU sponges

The host PU sponge was pre-treated with spray adhesive and bonded with the powder by sift-deposition method. In the SEM images, one can see that the of branch surfaces of naked sponge is smooth, while the surface of coated filter paper displayed a rough network frame that was covered by numerous flower-like FOTS-TiO_2 particles.

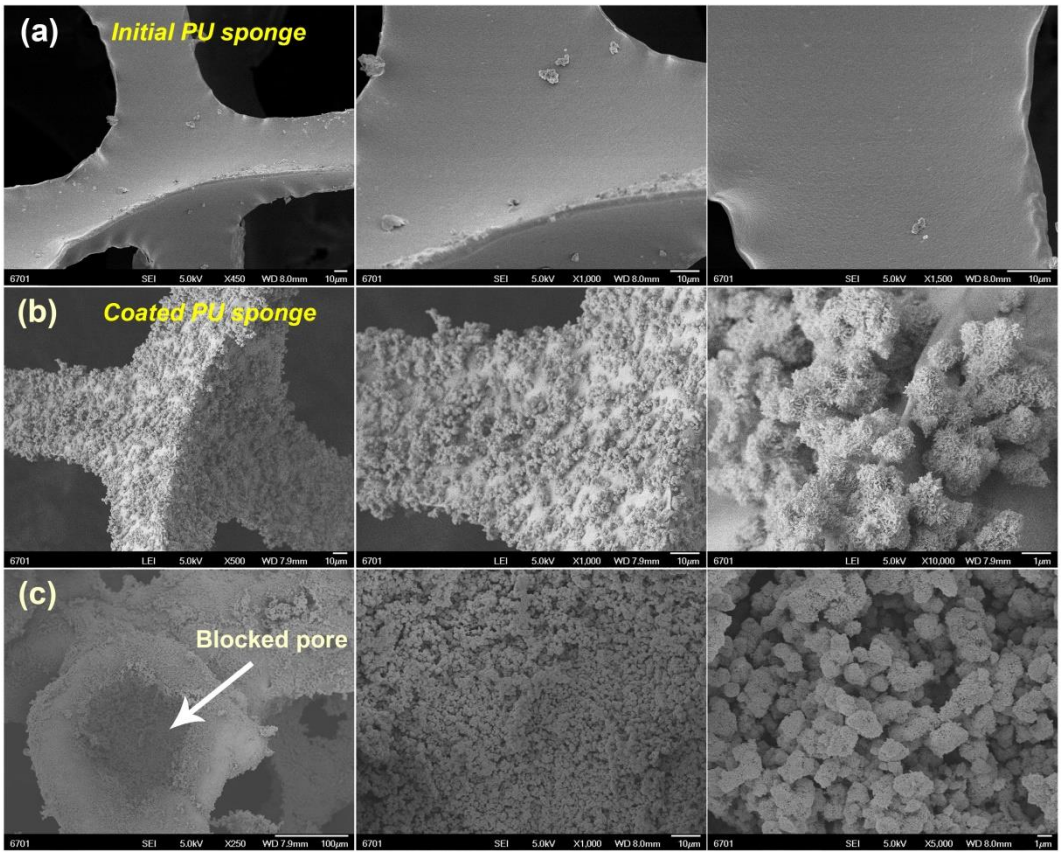

Fig. S6: Top-view SEM images of (a) initial and (b, c) FOTS-TiO_2-coated PU sponges.

5.4. SEM data of initial and coated cotton wools

The initial cotton was pre-treated with spray adhesive and bonded with the powder by sift-deposition method. SEM images of initial cotton fiber showed interlaced smooth fibers, while SEM images of coated cotton fiber displayed that the interlaced fibers were decorated with plenty of flower-like FOTS-TiO_2 particles.

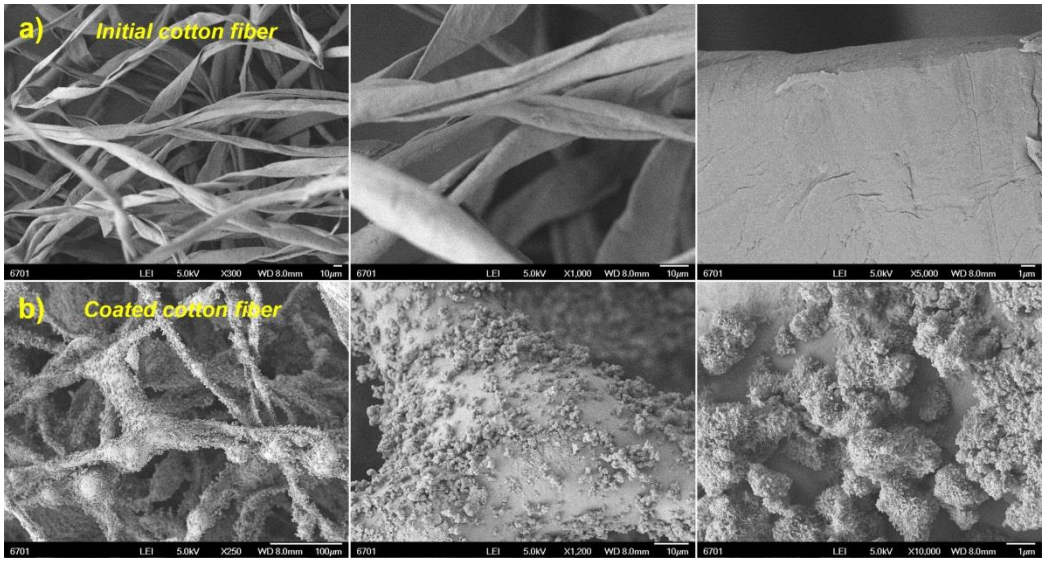

Fig. S7: Top-view SEM images of (a) initial and (b) FOTS-TiO_2-coated cotton fibers.

6. Self-cleaning and anti-fouling test with melting dusty snow

A special self-cleaning and anti-fouling test was performed using contaminated snow. On the glass surface, the FOTS-TiO_2 powder was bonded with double-sided tape at specific areas to form an enclosed hydrophilic area. The contaminated snow was placed onto the whole glass surface, and the self-cleaning and anti-fouling performance was observed during melting. As a result, during snow melting, the melted liquid water comes together to the untreated hydrophilic area with the dark contaminant, and coated areas were still kept clean.

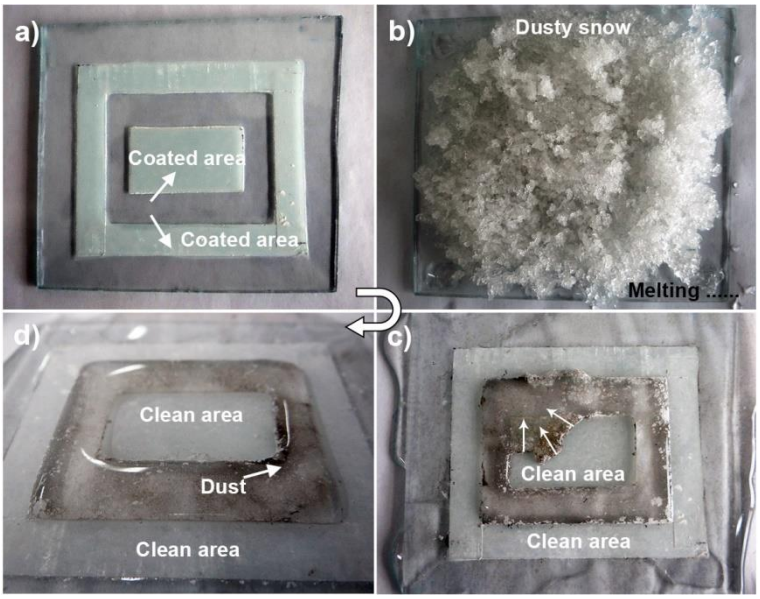

Fig. S8: Self-cleaning and anti-fouling property of the FOTS-TiO_2 coating under melting dusty snow. (a) A glass plate pretreated with FOTS-TiO_2 powder in specific areas. The bright white areas are coated with FOTS-TiO_2 powder using two-sided tape. (b) Dusty snow placed on the treated glass and kept at ~25°C. (c) The flow front of melted snow and dust. (d) Final state of water and dark contaminant on the treated glass plate.

7. Liquid marbles

When the water marbles were released onto the water surface one by one, the marbles can float and move on the water surface without collapse. As a result, a layer of close-packed water marbles with different size ranged from 6 μL to 20 μL can stably floated on the water surface. More than 50 water marbles are allowed to float on the water surface without disruption. This manifestation implies the great superhydrophobicity of water marbles and FOTS-TiO_2 powder.

To further demonstrate the great superamphiphobicity of FOTS-TiO_2 powder and the liquid marbles by using liquids with different surface tension, they are investigated to some extent. When the water, colza oil and glycerol droplets (~6 μL) are placed on a thin powder layer that is supported by water surface, they can keep perfectly spherical shapes on such a water-supported thin powder layer without falling down to the water layer. The marbles formed using water, colza oil and glycerol droplets are displayed on a sponge surface in a stable state. In addition, we observed the contact angle and shape of glycerol marble changing with the liquid volume (20 μL, 40 μL and 60 μL). From the pictures, one can see that the marble radii in horizontal direction (R_O) and vertical direction (R_V) are spontaneously increased, as well as the ratio of R_O: R_V. Otherwise, the marble contact angles have no significant change ($\theta \approx 150°$).

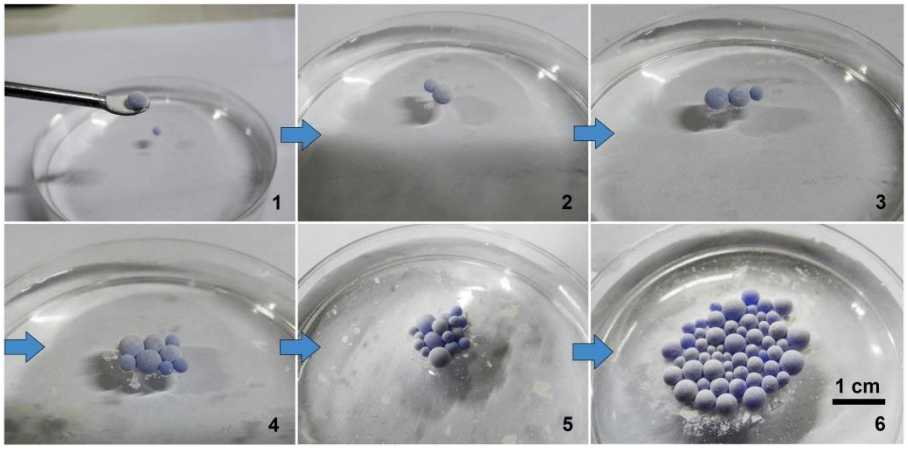

Fig. S9: Optical photographs of liquid water marbles floating on the water surface without disruption. The water marbles are released onto the water surface one by one.

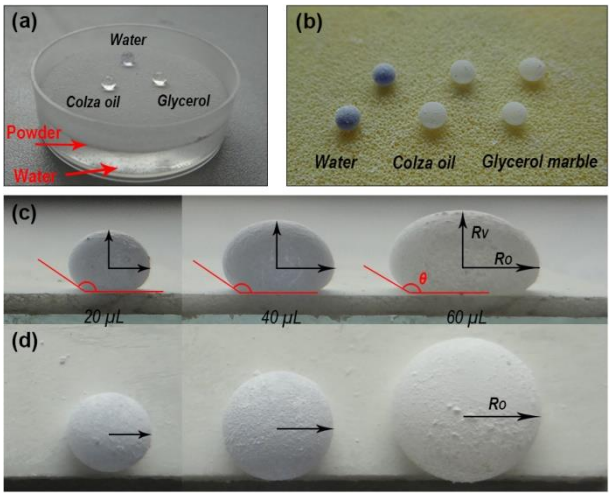

Fig. S10: (a) The state of water, colza oil and glycerol droplets on the water-supported thin powder layer. The droplets can keep perfectly spherical shapes on thin powder layer without falling down to the water layer, showing the stability of superamphiphobic powder. (b) Water, colza oil and glycerol marbles staying on a sponge. (c) Side-view and (d) top-view photographs of glycerol marbles with different liquid volumes of 20 μL, 40 μL and 60 μL. From the pictures, one can see that the marble radii in horizontal direction (R_O) and vertical direction (R_V) are spontaneously increased, as well as the ratio of R_O: R_V. Otherwise, the marble contact angles have no significant change ($\theta \approx 150°$).

8. Magnetic Fe_3O_4&FOTS-TiO_2 liquid marbles and dried composite particles

With the superamphiphobic FOTS-TiO_2 powder, a group of magnetic liquid marbles was prepared by wrapping a layer of powder on the surfaces of Fe_3O_4 aqueous droplets. After drying, wrinkled Fe_3O_4&FOTS-TiO_2 particles were formed, which can be attracted by a magnet. Due to faster water evaporation on the top of liquid marbles, the marbles shrank from the top and resulted in wrinkled particles. These magnetic Fe_3O_4&FOTS-TiO_2 liquid marbles and dried particles can be controlled and moved through moving a magnet at the bottom, showing strong magnetism and magnetic controllability.

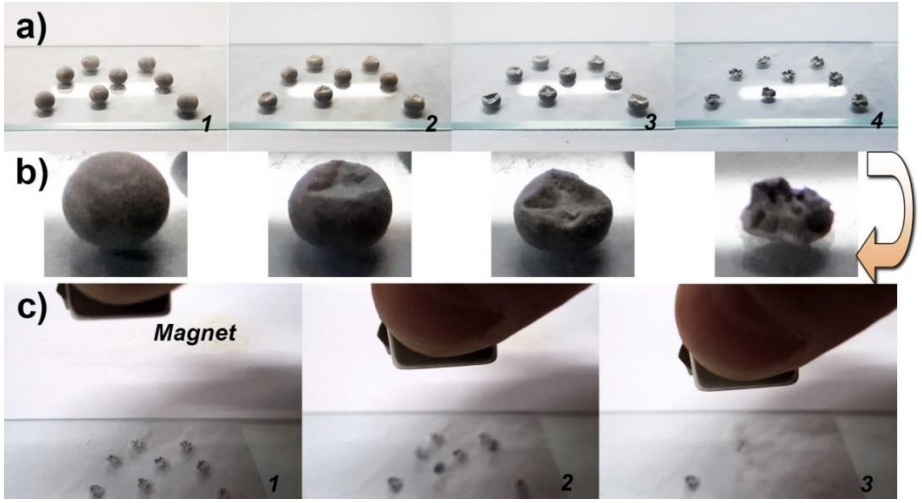

Fig. S11: Preparation of magnetic Fe_3O_4&FOTS-TiO_2 liquid marbles and particles. (a−b) The process from liquid marbles to dried particles during drying. (c) Magnetic test of prepared Fe_3O_4&FOTS-TiO_2 particles with a magnet.

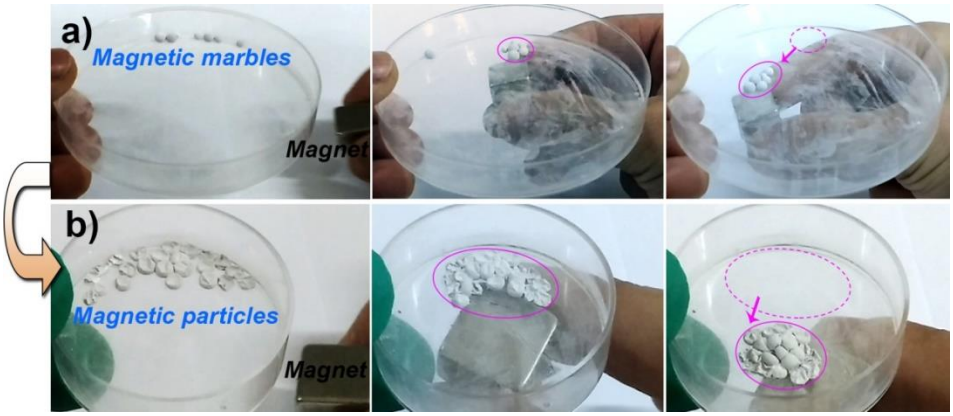

Fig. S12: Magnetic control of magnetic (a) liquid marbles and (b) dried composite particles. The dashed area is original position of liquid marbles (or dried composite particles).